

University of Groningen

## PKPD Modeling and Dosing Considerations in Advanced Ovarian Cancer Patients Treated with Cisplatin-Based Intraoperative Intraperitoneal Chemotherapy

Xie, Feifan; Van Bocxlaer, Jan; Colin, Pieter; Carlier, Charlotte; Van Kerschaver, Olivier; Weerts, Joseph; Denys, Hannelore; Tummers, Philippe; Willaert, Wouter; Ceelen, Wim

*Published in:*  
Aaps journal

*DOI:*  
[10.1208/s12248-020-00489-2](https://doi.org/10.1208/s12248-020-00489-2)

**IMPORTANT NOTE: You are advised to consult the publisher's version (publisher's PDF) if you wish to cite from it. Please check the document version below.**

*Document Version*  
Publisher's PDF, also known as Version of record

*Publication date:*  
2020

[Link to publication in University of Groningen/UMCG research database](#)

### *Citation for published version (APA):*

Xie, F., Van Bocxlaer, J., Colin, P., Carlier, C., Van Kerschaver, O., Weerts, J., Denys, H., Tummers, P., Willaert, W., Ceelen, W., & Vermeulen, A. (2020). PKPD Modeling and Dosing Considerations in Advanced Ovarian Cancer Patients Treated with Cisplatin-Based Intraoperative Intraperitoneal Chemotherapy. *Aaps journal*, 22(5), [96]. <https://doi.org/10.1208/s12248-020-00489-2>

### **Copyright**

Other than for strictly personal use, it is not permitted to download or to forward/distribute the text or part of it without the consent of the author(s) and/or copyright holder(s), unless the work is under an open content license (like Creative Commons).

The publication may also be distributed here under the terms of Article 25fa of the Dutch Copyright Act, indicated by the "Taverne" license. More information can be found on the University of Groningen website: <https://www.rug.nl/library/open-access/self-archiving-pure/taverne-amendment>.

### **Take-down policy**


If you believe that this document breaches copyright please contact us providing details, and we will remove access to the work immediately and investigate your claim.

Downloaded from the University of Groningen/UMCG research database (Pure): <http://www.rug.nl/research/portal>. For technical reasons the number of authors shown on this cover page is limited to 10 maximum.



## Research Article

# PKPD Modeling and Dosing Considerations in Advanced Ovarian Cancer Patients Treated with Cisplatin-Based Intraoperative Intraperitoneal Chemotherapy

Feifan Xie,<sup>1,2,10</sup>  Jan Van Bocxlaer,<sup>2</sup> Pieter Colin,<sup>2,3</sup> Charlotte Carlier,<sup>4,5</sup> Olivier Van Kerschaver,<sup>6</sup> Joseph Weerts,<sup>7</sup> Hannelore Denys,<sup>5,8</sup> Philippe Tummers,<sup>9</sup> Wouter Willaert,<sup>4</sup> Wim Ceelen,<sup>4,5</sup> and An Vermeulen<sup>2</sup>

Received 11 June 2020; accepted 16 July 2020

**Abstract.** Intraperitoneal chemoperfusion (IPEC) of cisplatin is a popular treatment for advanced ovarian cancer, typically under hyperthermia (HIPEC). The use of cisplatin under (H)IPEC is off-label, and the role of hyperthermia is unknown. The aim of this study was to characterize the pharmacokinetic/pharmacodynamic (PKPD) properties of cisplatin under (H)IPEC and to predict the optimal treatment regimen. Using a randomized design, data on intact cisplatin perfusate and plasma concentrations, leukocyte counts—a hematotoxicity marker—and serum creatinine—a nephrotoxicity marker—were collected from 50 patients treated with a combination of cytoreductive surgery (CRS) and either normothermic or hyperthermic IPEC of cisplatin dosed at 75, 100, and 120 mg/m<sup>2</sup>. The non-linear mixed effects modeling technique was used to construct the PKPD models. The PK of intact cisplatin was characterized by a two-compartment model. A semi-physiological myelosuppression model for the leukopenia was modified to account for the CRS-induced leukocytosis and the residual myelosuppression effect of neoadjuvant chemotherapy. The incidence and severity of nephrotoxicity were described by a discrete-time Markov model. Hyperthermia increased the absorption rate of cisplatin by 16.3% but did not show a clinically relevant impact on the investigated toxicities compared with normothermia. Leukopenia was not severe, but nephrotoxicity can become severe or life-threatening and was affected by the dose and IPEC duration. The model predicted that nephrotoxicity is minimal at a cisplatin dose of 75 mg/m<sup>2</sup> with an IPEC duration of 1–2 h and an 1-h duration is favored for doses between 100 and 120 mg/m<sup>2</sup>.

**KEY WORDS:** cisplatin; HIPEC; ovarian cancer; PKPD; NONMEM.

## INTRODUCTION

Ovarian cancer ranks eighth in cancer deaths among women and is the deadliest gynecologic cancer (1). More than two-thirds of the patients receive a diagnosis of advanced

FIGO (International Federation of Gynecology and Obstetrics) stage III or IV disease with peritoneal carcinomatosis (PC) (2–4). The standard treatment for advanced ovarian cancer involves primary cytoreductive surgery (CRS) followed by six cycles of adjuvant chemotherapy with

**Electronic supplementary material** The online version of this article (<https://doi.org/10.1208/s12248-020-00489-2>) contains supplementary material, which is available to authorized users.

<sup>1</sup> Division of Biopharmaceutics and Pharmacokinetics, Xiangya School of Pharmaceutical Sciences, Central South University, Tongzipo Road 172, Changsha, 410013, China.

<sup>2</sup> Laboratory of Medical Biochemistry and Clinical Analysis, Faculty of Pharmaceutical Sciences, Ghent University, Ottergemsesteenweg 460, 9000, Ghent, Belgium.

<sup>3</sup> Department of Anesthesiology, University Medical Center Groningen, University of Groningen, Hanzeplein 1, 9713 GZ, Groningen, The Netherlands.

<sup>4</sup> Department of GI Surgery, Ghent University Hospital, 9000, Ghent, Belgium.

<sup>5</sup> Cancer Research Institute Ghent (CRIG), 9000, Ghent, Belgium.

<sup>6</sup> Department of Surgery, St. Lucas Andreas Hospital, 9000, Ghent, Belgium.

<sup>7</sup> Department of Surgery, CHC, Liège, Belgium.

<sup>8</sup> Department of Medical Oncology, Ghent University Hospital, 9000, Ghent, Belgium.

<sup>9</sup> Department of Gynecology, Ghent University Hospital, 9000, Ghent, Belgium.

<sup>10</sup> To whom correspondence should be addressed. (e-mail: feifan.xie@csu.edu.cn)

intravenous carboplatin and paclitaxel (2,5,6). If a primary CRS is not deemed feasible, three cycles of neoadjuvant chemotherapy are proposed, followed by interval CRS and three cycles of adjuvant chemotherapy (2,6). Although the initial response to this standard of care is high (60–80%), most patients (75%) will eventually develop recurrent peritoneal disease, which arises from peritoneal minimal residual disease (pMRD), remaining post CRS (2,7).

Since ovarian cancer usually remains confined to the peritoneal cavity, the use of intraperitoneal chemotherapy has pharmacokinetic (PK) advantages for achieving high tumor drug exposure (2). Intraoperative intraperitoneal chemoperfusion (IPEC) is a frequently used type of intraperitoneal chemotherapy. The advantage of IPEC, as opposed to systemic chemotherapy, is the possibility to achieve optimal chemotherapy exposure of all peritoneal surfaces at risk while simultaneously minimizing systemic exposure, consequently resulting in potentially increased efficacy and low systemic drug-related toxicity (3,8). IPEC can be delivered under normothermic (37°C) or more often under hyperthermic (41–43°C, termed as HIPEC) conditions.

The commonly used drugs with (H)IPEC are platinum derivatives (e.g., cisplatin, carboplatin, and oxaliplatin) and taxanes (e.g., paclitaxel and docetaxel), previously demonstrated to be highly effective as intravenous chemotherapy for ovarian cancer (9,10). Among the platinum derivatives, cisplatin is the most widely used agent for HIPEC treatment of PC of ovarian origin because of its very strong cytotoxic effect on ovarian cancer cells, and a demonstrated synergistic effect with hyperthermia in *in vitro* cell experiments (11–13). Cisplatin is a highly toxic drug with a narrow therapeutic index. Following administration, cisplatin is vulnerable to deactivation by biological nucleophiles in the bloodstream, forming “fixed” (binding with high molecular mass substances, such as albumin) and “mobile” (binding with low molecular mass substances, such as glutathione and methionine) biologically inactive metabolites (14,15). The intact cisplatin that enters tumor cells undergoes hydrolysis and then interacts with DNA, inducing programmed cell death (16). Intact cisplatin may cause side effects, including nephrotoxicity, hematological toxicity, nausea and vomiting, ototoxicity, and neurotoxicity (17,18). Of these, nephrotoxicity is the major dose-limiting side effect.

The use of cisplatin under (H)IPEC is off-label, based on the approved intravenous injection route. Due to the lack of a standard treatment regimen, the current reported (H)IPEC doses of cisplatin range from 50 to as high as 250 mg/m<sup>2</sup> with treatment durations varying from 30 to 120 min (7,19–21). Moreover, the pharmacokinetics (PK) and drug responses (i.e., efficacy and toxicity) of cisplatin (H)IPEC dosing, and their potential relationships are poorly understood. The popular use of total platinum (i.e., all platinum species) or ultrafilterable platinum (cisplatin and its “mobile” metabolites) for PK analysis may further blur our understanding of the pharmacokinetic/pharmacodynamic (PKPD) since these species are a mixture of platinum derivatives with greatly differing activities and toxicities (22,23). Lastly, conflicting results about the benefit of hyperthermia compared with normothermia were reported for cisplatin (24–26). These issues are likely to expose patients to an uncertain benefit/risk outcome under (H)IPEC.

The aim of this study was to characterize the PK of intact cisplatin under hyperthermic and normothermic IPEC, to explore the quantitative relationships between PK and adverse effects, and finally to predict the optimal treatment regimen by means of a mixed effects modeling and simulation approach.

## MATERIALS AND METHODS

### Study Design and Ethics

This was a prospective, multicenter, randomized phase 2 trial. In the first part of the trial (24 patients), four treatment arms were tested: group 1 was treated with an IPEC dose of 75 mg/m<sup>2</sup> cisplatin at 37°C, group 2 with an IPEC dose of 75 mg/m<sup>2</sup> cisplatin at 41°C, group 3 with an IPEC dose of 120 mg/m<sup>2</sup> cisplatin at 37°C, and group 4 with an IPEC dose of 120 mg/m<sup>2</sup> cisplatin at 41°C. In the second part of the randomized trial (26 patients), the dose of 120 mg/m<sup>2</sup> was reduced to 100 mg/m<sup>2</sup> due to nephrotoxicity concerns, while other conditions were kept the same as the first part. The study protocol was reviewed and approved by the institutional review board of Ghent University Hospital. The trial was registered at [ClinicalTrials.gov](https://clinicaltrials.gov) (identifier: NCT02567253) and European Clinical Trials Database (EudraCT) (number: 2015-000418-23). All enrolled patients provided written informed consent.

Inclusion criteria were biopsy-proven primary or recurrent epithelial ovarian carcinoma (FIGO stage III or IV) or primary peritoneal carcinoma, age of 18 years or higher, complete or nearly complete macroscopic cytoreduction (< 2.5 mm, completeness of cytoreduction score CC-0 or CC-1) at the time of possible surgery, platinum sensitive disease, not pregnant or breastfeeding, no major cardiac or respiratory deficiency, no other concurrent malignant diseases, absent or limited (< 500 ml) clinical ascites, acceptable bone marrow function (defined as platelet count > 100,000/μl, hemoglobin > 9 g/dl, and neutrophil granulocytes > 1500/ml), normal liver and renal function, and good performance status (Karnofsky index > 70%).

Exclusion criteria included as follows: severe or uncontrolled cardiac insufficiency, including recent (< 6 months) occurrence of myocardial infarction, the presence of congestive cardiac insufficiency, the presence of symptomatic angor in spite of optimal medical care, the presence of cardiac arrhythmia requiring medical treatment presenting insufficient rhythm control, or uncontrolled arterial hypertension; active bacterial, viral, or fungal infection; active gastroduodenal ulcer; uncontrolled diabetes mellitus; tumor in the presence of bowel obstruction; and a peritoneal cancer index ≥ 25.

### Cytoreductive Surgery and Intraperitoneal Chemoperfusion

If the tumor has disseminated across the whole abdomen, making optimal primary CRS occasionally hard to accomplish, neoadjuvant chemotherapy (NACT) (systemic carboplatin area under the curve [AUC] 6 mg/ml per min and paclitaxel 80 mg/m<sup>2</sup>) was given with the aim given to reduce tumor load and minimize postoperative complications. Often, a minimal waiting period of 2 to 3 weeks (judged by

the clinicians) was respected between the last dose of neoadjuvant chemotherapy and the date of CRS.

Patients underwent primary or interval CRS aiming at complete or near complete cytoreduction (CC-0 or CC-1). When optimal cytoreduction was deemed feasible, patients were randomized in the operating theater to a specific treatment group regarding dose and temperature, using opaque sealed envelopes. IPEC was performed for 90 min using the open (coliseum) technique. Cisplatin was dissolved in a balanced peritoneal dialysis solution (Physioneal™ 1.36, Baxter, The Netherlands), and the volume of perfusate was calculated as 2 l per m<sup>2</sup> body surface area (BSA). Systemic sodium thiosulfate was given over 20 min from the start of the chemoperfusion (4 g/m<sup>2</sup>, dissolved in 150 ml 0.9% NaCl) and during 6 h after completion of the chemoperfusion (12 g/m<sup>2</sup>, dissolved in 1000 ml 0.9% NaCl) in order to prevent nephrotoxicity from cisplatin.

### Sample Collection and Measurement

Perfusate samples were taken after one circulation of the chemoperfusion through the abdomen (time = 3–5 min), and at 45 and 90 min (end of chemoperfusion). Blood samples were drawn before chemoperfusion (0 min); 0.25, 0.5, and 1.5 (end of chemoperfusion); and 2, 3, 7.5, and 24 h after the start of the chemoperfusion. Blood samples were immediately centrifuged to obtain plasma. The perfusate and plasma samples were stored at –80°C until analysis. The concentrations of unchanged cisplatin were measured using a previously developed UPLC-MS/MS method (27). The lower limit of quantification (LLOQ) of intact cisplatin in plasma was 20 ng/ml. The method imprecision was less than 7.6% and bias was less than ±5.7%.

Blood samples for the measurement of leukocytes and serum creatinine were collected before surgery and on a daily basis (judged by the clinicians) up to 7 and 14 days post IPEC to monitor nephrotoxicity and hematological toxicity, respectively.

### Pharmacokinetic/Pharmacodynamic Analysis

Non-linear mixed effects modeling was used to construct the population PK and PKPD models of cisplatin. The PK modeling was based on cisplatin concentrations in perfusate and plasma, hematological toxicity modeling was based on the continuous data of leukocytes using the semi-mechanistic myelosuppression model introduced by Friberg *et al.* (28) (shown by the light blue blocks in the bottom part of Fig. 1) as a starting model, and nephrotoxicity modeling was based on ordered categorical data of serum creatinine. The details about the strategy for model development are provided in Supplemental 1.

### Model-Based Simulations

Stochastic simulations were carried out based on the developed PKPD models to determine the optimal IPEC treatment regimen with minimal toxicities. Single doses of 75, 100, and 120 mg/m<sup>2</sup> under three different typical IPEC durations (i.e., 60, 90, and 120 min) were investigated. For

each scenario, 1000 virtual patients were simulated to calculate the incidence of toxicity.

## RESULTS

### Patient Characteristics

From March 2016 to September 2019, 50 eligible patients were included and completed the study. Patient demographics and clinical characteristics are summarized in Table I. Among these patients, 26 patients received a dose of 75 mg/m<sup>2</sup>, 12 patients had a dose of 100 mg/m<sup>2</sup>, and 12 patients had a dose of 120 mg/m<sup>2</sup>. Twenty-five patients received IPEC dosing at 37°C, and the other 25 patients were given IPEC dosing at 41°C. Twelve patients (24%) experienced drug-induced nephrotoxicity (CTCAE grades 1–4). Before CRS, 5 patients (10%) had leukopenia (CTCAE grades 1–3, 1.0–3.0 × 10<sup>9</sup> cells/l) due to the residual myelosuppression effect of NACT.

### Pharmacokinetic/Pharmacodynamic Analysis

*Population Pharmacokinetics.* A total of 144 cisplatin perfusate and 270 plasma concentrations were available to characterize cisplatin pharmacokinetics in ovarian cancer patients treated with IPEC after CRS. The population pharmacokinetics analysis demonstrated that the absorption of cisplatin from the peritoneum to blood was well described by a first-order absorption with a short absorption lag time. The lag time accounted for the delivery time of drug solutions from the reservoir into the abdominal cavity, and this substantially decreased the objective function value ( $\Delta$ OFV of –54.2). The plasma concentrations were best described by a two-compartment disposition model with first-order elimination from the central compartment. A high correlation (correlation coefficient: 0.90) was found between the central volume of distribution ( $V_c$ ) and systemic clearance (CL) ( $\Delta$ OFV of –43.4). Of all tested covariates, only the temperature was found influential ( $\Delta$ OFV of –7.3) on the first-order absorption rate constant ( $k_a$ ). The  $k_a$  for HIPEC was 16.3% higher than for the normothermic IPEC, resulting in a 10.8% higher predicted cisplatin peak plasma concentration ( $C_{max}$ ). The effect of hyperthermia for the following hematological toxicity and nephrotoxicity analysis was then evaluated on top of the effect it has on the PK of cisplatin.

A schematic representation of the final PK structural model is depicted by the gray blocks (upper left) in Fig. 1. The parameter estimates of the final PK model and associated uncertainties are presented in Table II. Diagnostic plots for the final PK model are shown in Fig. 2 and Figs. S1–2 in Supplemental 2.

*Semi-physiological Modeling of Hematological Toxicity.* A total of 488 leukocyte measurements were used to characterize the time course of leukocytes in ovarian cancer patients receiving cisplatin-based IPEC post CRS. As shown in Fig. 3a, the typical time course of leukocytes comprised an initial sharp peak (within 24 h after CRS), followed by the nadir around day 5, then followed by a rebound peak around days 9–10, and finally a gradual re-attainment of the baseline value. The transient increase in leukocyte numbers was likely due to surgical stress, as

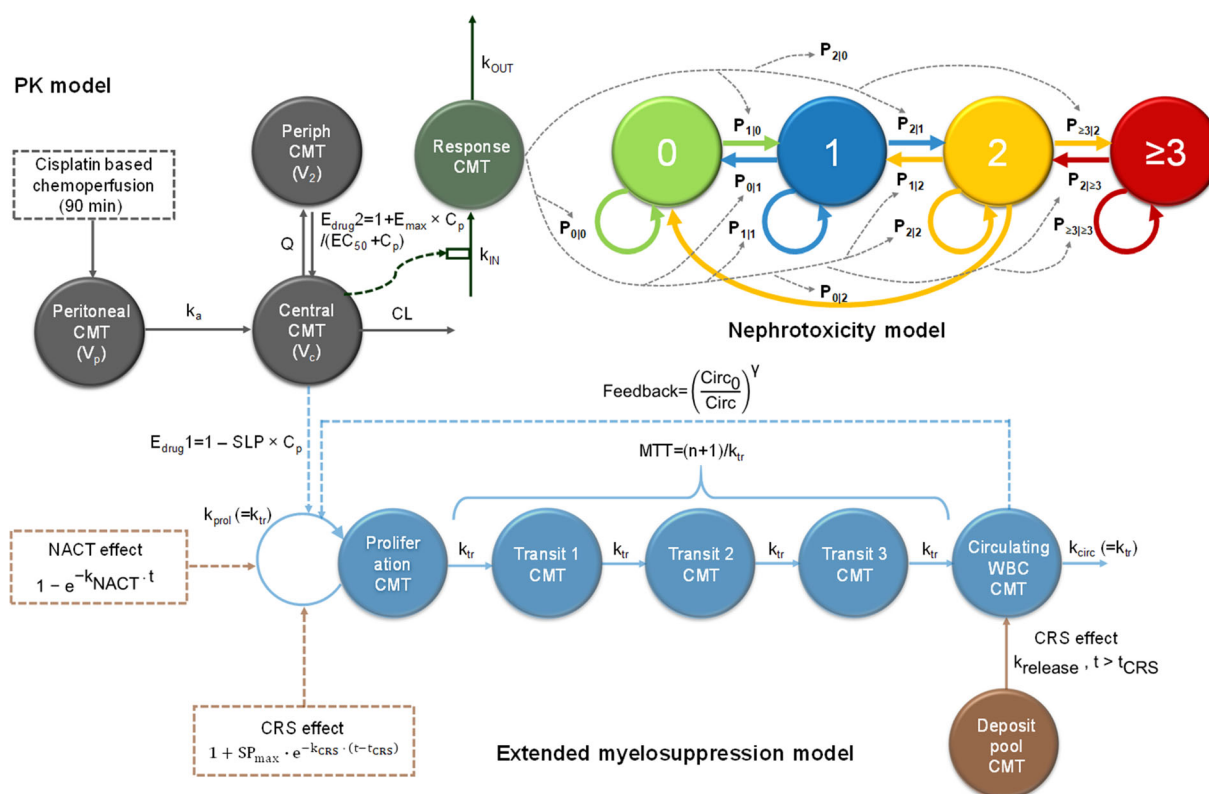


**Fig. 1.** Graphical representation of the structure of the final population pharmacokinetics model (gray blocks in the upper left), extended myelosuppression model (light blue and brown blocks in the bottom part of the figure), and nephrotoxicity model (upper right part of the figure). The gray arrows shown in the nephrotoxicity model indicate that the transition probabilities between different grades are influenced by the *response* (*t*) derived from the indirect response model of cisplatin

previously reported for neutrophils (29,30). NACT is thought to be the cause for the patients with leukopenia before surgery as these patients received the last dose of NACT within 1.5–4 weeks before CRS. After (H)IPEC, six

**Table I.** Demographics and Clinical Characteristics of the Study Patients (*n* = 50)

Characteristics	<i>n</i> (%) or median (interquartile range)		
	Entire population	Normothermic patient	Hyperthermic patient
Dose regimen (mg/m <sup>2</sup> )			
75	26 (52.0%)	13 (26.0%)	13 (26.0%)
100	12 (24.0%)	6 (12.0%)	6 (12.0%)
120	12 (24.0%)	6 (12.0%)	6 (12.0%)
Age (years)	61 (57–67)	61 (55–67)	61 (59–69)
Body weight (kg)	70 (61–76)	70 (62–76)	66 (61–76)
Body mass index (kg/m <sup>2</sup> )	24.7 (22.4–28.7)	25.7 (22.7–29.4)	24.5 (22.4–27.6)
Body surface area (m <sup>2</sup> )	1.8 (1.7–1.9)	1.8 (1.7–1.9)	1.7 (1.6–1.9)
Serum creatinine (mg/dl)	0.72 (0.59–0.79)	0.65 (0.57–0.76)	0.76 (0.66–0.84)
Creatinine clearance (Cockcroft and Gault, ml/min)	88.4 (71.6–112)	99.2 (78.8–117.2)	85.0 (61.7–105.5)
Neoadjuvant chemotherapy (NAC) regimen			
None	5 (10.0%)	2 (4.0%)	3 (6.0%)
IV carboplatin AUC6 and paclitaxel 80 mg/m <sup>2</sup>	45 (90.0%)	23 (46.0%)	22 (44.0%)
Last dosing time (weeks) of NACT before surgery	4 (3–4)	4 (3.5–5)	3.5 (3–4)
Highest grade of nephrotoxicity during observation period			
Grade 1	6 (12.0%)	3 (6.0%)	3 (6.0%)
Grade 2	1 (2.0%)	0 (0%)	1 (2.0%)
Grade 3	4 (8.0%)	3 (6.0%)	1 (2.0%)
Grade 4	1 (2.0%)	0 (0%)	1 (2.0%)
Leukocytes (10 <sup>9</sup> cells/l) (before surgery)	5.46 (4.0–7.52)	5.02 (3.46–7.16)	6.08 (4.32–7.47)

**Table II.** Parameter Estimates of the Final Pharmacokinetic Model and the Results of the Sampling Importance Resampling (SIR) Approach

Parameter	Estimate (RSE %) <sup>a</sup> (Shrinkage %)	Meaning of parameters
<b>Fixed effects</b>		
ALAG1 (h)	0.0140 (13.3)	Delivery time of drug solution from reservoir into the abdominal cavity
$k_a = \theta_{ka} \times (1 + \theta_{TEMP})$		First-order absorption rate constant
$\theta_{ka}$ (h <sup>-1</sup> )	1.12 (8.1)	$k_a$ of patients with chemoperfusion at 37°C
$\theta_{TEMP}$ (41°C)	0.163 (15.9)	Hyperthermia (41°C) effect on $k_a$
$V_p$ (l)	4.83 (8.7)	Perfusate volume in abdomen
CL (l/h)	44.3 (11.7)	Clearance
$V_c$ (l)	16.0 (13.9)	Central volume of distribution
$Q$ (l/h)	31.0 (14.6)	Inter-compartmental clearance
$V_2$ (l)	12.5 (11.9)	Peripheral volume of distribution
<b>Inter-individual variability (IIV) (%CV)</b>		
$k_a$	23.4 (24.6) [12.1]	
$V_p$	27.3 (24.3) [12.0]	
CL	52.8 (22.3) [9.90]	
$V_c$	86.9 (23.2) [11.5]	
$\omega_{CL,Vc}$	0.336 (10.0)	Covariance between the variances of CL and $V_c$
$Q$	47.6 (15.0) [35.4]	
<b>Residual variability</b>		
Proportional error <sup>b</sup> (perfusate, %)	20.1 (14.2) [30.0]	
Proportional error <sup>b</sup> (plasma, %)	31.3 (11.4) [20.7]	

CV (%) is calculated according to  $CV (\%) = \sqrt{\exp(\omega^2) - 1} \times 100\%$ .  $\omega^2$ , the variance estimate in the log domain

<sup>a</sup> RSE, relative standard error, obtained from SIR

<sup>b</sup> An additive error model in the log-transformed domain was used to characterize the residual unexplained variability, which approximates to a proportional error in the normal domain

patients (12%) experienced a short period ( $\leq 48$  h) of grade 1 (four patients who had normal baseline leukocytes and one patient who had abnormal baseline leukocytes) or grade

2 (one patient who had leukopenia before surgery) leukopenia. No grade 3 ( $> 100.0 \times 10^9$  cells/l) leukocytosis was observed.

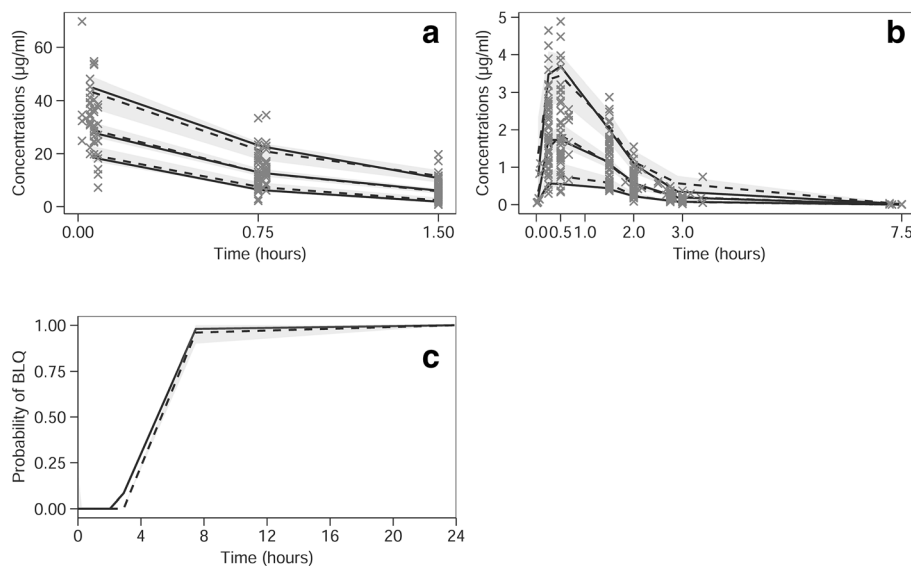


**Fig. 2.** Prediction-corrected visual predictive checks for the final population pharmacokinetics model of cisplatin perfusate (a) and plasma (b, c) concentrations. For panels a and b: The solid lines are the observed percentiles (5, 50, and 95th percentiles). The dashed black lines are predicted percentiles, and the shaded areas are the corresponding 95% confidence intervals on the predicted percentiles. For panel c: The black solid line represents the median of the observations, and the black dashed line represents the median of the model predictions. The gray shaded area represents the 90% prediction interval. BLQ, below the limit of quantification

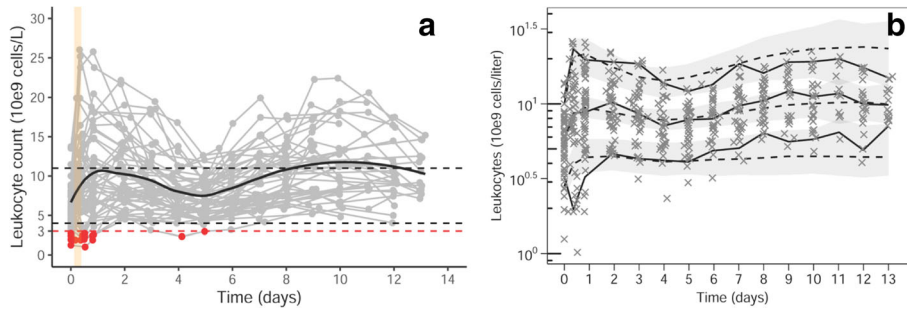


**Fig. 3.** The time course of leukocytes and model predictions *versus* observations in patients receiving cytoreductive surgery and cisplatin-based intraoperative chemoperfusion. Panel **a** shows the time course of leukocyte observations: The zero time point indicates the starting time of cytoreductive surgery, while the shaded yellow area represents the starting time interval of chemoperfusion. The black dashed lines display the normal range ( $4.0\text{--}11.0 \times 10^9$  cells/l) of leukocytes in man. The black solid line represents a Loess smoother. Patients experienced leukopenia ( $\geq$  grade 1) if they had leukocyte measurements below the red dashed line ( $3.0 \times 10^9$  cells/l). Panel **b** displays the prediction-corrected visual predictive checks for the final myelosuppression model: The solid lines are the observed percentiles (5, 50, and 95th percentiles). The dashed black lines are predicted percentiles, and the shaded areas are the corresponding 95% confidence intervals on the predicted percentiles. A base 10 logarithmic scale was used for the  $y$ -axis. The observed 5th percentile line falls outside the prediction intervals for the first day; this was mainly driven by the points being affected by the residual myelosuppressive effect

As the original myelosuppression model proposed by Friberg *et al.* does not describe the transient increase in leukocytes induced by CRS, the model was extended by adding a deposit compartment representing the stored mature leukocytes within the bone marrow sinusoids. CRS was assumed to initialize the mobilization of leukocytes from the deposit compartment to the circulating compartment ( $\Delta\text{OFV} = -155.6$ ) and increase the mitosis rate of proliferative cells ( $\Delta\text{OFV} = -64.9$ ). The mobilization of leukocytes was modeled as a first-order release from the estimated initial number of cells in the deposit compartment. The CRS effect on the proliferation rate was modeled by a stimulatory function and its effect was exponentially declining over time. A residual myelosuppressive effect of the NACT was added on the proliferation rate, implemented as an exponentially declining function, for patients with leukopenia before surgery to ascertain a physiologically reasonable model prediction of baseline leukocyte counts once all treatment effects had worn out ( $\Delta\text{OFV} = -26.9$ ). A linear cisplatin concentration-effect relationship on the proliferation rate of

the leukocytes best fitted the data. No significant improvement of the model fit was found by increasing the numbers of transit compartments or using other drug effect functions (e.g.,  $E_{\text{max}}$  and sigmoid  $E_{\text{max}}$  models). The data did not support the estimation of  $k_{\text{circ}}$  (disappearance rate constant of leukocytes from the circulation pool); thus, it was assumed in the modeling that  $k_{\text{circ}}$  equals  $k_{\text{tr}}$  (transition rate constant describing cell transfer between transit compartments).

In the final model, the CRS effect on the mobilization of leukocytes from the deposit compartment is according to Eq. 1, and the residual myelosuppressive effect of NACT, the CRS effect, the myelosuppressive effect of IPEC (only for patients with leukopenia before surgery), and the feedback loop on the proliferation rate are shown in Eq. 2.

$$\frac{d\text{Deposit}}{dt} = \begin{cases} 0, & \text{if } t \leq t_{\text{CRS}} \\ -k_{\text{release}} \cdot \text{Deposit}(t), & \text{if } t > t_{\text{CRS}} \end{cases} \quad (1)$$

$$k_{\text{prol}} = \begin{cases} k_{\text{prol}(0)} \cdot \left(\frac{\text{Circ}_0}{\text{Circ}}\right)^\gamma, & \text{if } t = 0 \text{ (i.e., before start of NACT); Circ}_0 = \text{Circ}(t = 0) \\ k_{\text{prol}(0)} \cdot \left(\frac{\text{Circ}_0}{\text{Circ}}\right)^\gamma \cdot (1 - \exp^{-k_{\text{NACT}} \cdot t}), & \text{if } t > 0 \text{ and } t \leq t_{\text{CRS}} \\ k_{\text{prol}(0)} \cdot \left(\frac{\text{Circ}_0}{\text{Circ}}\right)^\gamma \cdot (1 - \exp^{-k_{\text{NACT}} \cdot t}) \cdot (1 + \text{SP}_{\text{max}} \cdot \exp^{-k_{\text{CRS}} \cdot (t - t_{\text{CRS}})}), & \text{if } t > t_{\text{CRS}} \text{ and } t \leq t_{\text{IPEC}} \\ k_{\text{prol}(0)} \cdot \left(\frac{\text{Circ}_0}{\text{Circ}}\right)^\gamma \cdot (1 - \exp^{-k_{\text{NACT}} \cdot t}) \cdot (1 + \text{SP}_{\text{max}} \cdot \exp^{-k_{\text{CRS}} \cdot (t - t_{\text{CRS}})}) \cdot (1 - \text{SLP} \cdot C_p), & \text{if } t > t_{\text{IPEC}} \end{cases} \quad (2)$$

where  $\text{Deposit}(t)$  represents the amount of leukocytes at the deposit compartment, which starts to release to the bloodstream after the start of CRS ( $t_{\text{CRS}}$ ) with a first-order release

rate constant  $k_{\text{release}}$ ;  $k_{\text{prol}(0)}$  represents the first-order proliferation rate constant before the NACT treatment;  $\text{Circ}$  is the circulating observed leukocytes in blood, and  $\text{Circ}_0$  represents

the baseline blood leukocytes in the absence of treatment;  $\gamma$  is the feedback loop factor on the proliferation rate constant;  $k_{\text{NACT}}$  is the first-order disappearance rate constant of the residual myelosuppressive effect of the NACT;  $\text{SP}_{\text{max}}$  is the maximum stimulatory effect of CRS stress on  $k_{\text{prol}(0)}$ , which starts at the time of CRS ( $t_{\text{CRS}}$ );  $k_{\text{CRS}}$  is the first-order disappearance rate constant of the CRS stress effect on  $k_{\text{prol}(0)}$ ; SLP is the slope of the linear concentration-effect relationship of cisplatin, which begins at the initiation of IPEC ( $t_{\text{IPEC}}$ );  $C_p$  represents the individual cisplatin plasma concentration predicted from the population PK model.

The final myelosuppression model is represented by the light blue and brown blocks (bottom part) in Fig. 1. The NONMEM control stream of the final myelosuppression model is provided in Supplemental 3. The parameter estimates and associated uncertainties of the final model are shown in Table III. Diagnostic plots (panel b in Fig. 3 and Fig. S3 in Supplemental 2) and the representative individual fitting plots (Fig. S4 in Supplemental 2) demonstrated a good agreement of model predictions with the observed data.

**Nephrotoxicity Modeling.** Figure S5 in Supplemental 2 shows the transitions between observed toxicity states in patients who experienced nephrotoxicity. Since we only obtained the recorded nephrotoxicity data within the 7-day window, the toxicity extended beyond this timeframe was not considered. With the proportional odds model, an indirect response model best described the drug concentration-response relationship ( $\Delta\text{OFV}$  of  $-74.9$ ). This model generally characterized the nephrotoxicity observations well except for the grade  $\geq 3$  events (The VPC plot is shown as Fig. S6 in Supplemental 2). The addition of Markov element was then tested (five parameters were added on the “baseline logits”), and this resulted in a  $\Delta\text{OFV}$  of  $-151.0$  and an associated improvement of model fit. Theoretically, there are sixteen

different possible transitions between the four different toxicity grades (0, 1, 2, and  $\geq 3$ ). However, four transitions (i.e., from 0 to  $\geq 3$ , from 1 to  $\geq 3$ , from  $\geq 3$  to 1, and from  $\geq 3$  to 0) were not observed and hence not modeled to avoid overparameterization of the model. Among the predictors tested, the dose, AUC,  $C_{\text{max}}$ , and drug concentration over time all significantly improved the model fit. The drug concentration over time, implemented using an indirect response model with an  $E_{\text{max}}$  drug-effect function, showed the most profound relationship ( $\Delta\text{OFV}$  of  $-29.5$ ), compared with dose ( $\Delta\text{OFV}$  of  $-7.8$ ), AUC ( $\Delta\text{OFV}$  of  $-8.4$ ), and  $C_{\text{max}}$  ( $\Delta\text{OFV}$  of  $-9.7$ ). After the implementation of drug concentration over time, no further improvement in the description of the data was observed when other predictors (e.g., dose, AUC,  $C_{\text{max}}$ , and temperature effect) were incorporated. No IIV on any of the parameters was found significant.

The influence of the drug effect on the transition probability  $f_{k_j|k_{j-1}}$  in the final model is described using Eqs. 3–4. The structure of the final nephrotoxicity model is depicted in the upper right blocks in Fig. 1, and the NONMEM control stream for this model is provided in Supplemental 3.

$$\frac{d\text{Response}}{dt} = K_{\text{IN}} \cdot \left( 1 + E_{\text{max}} \cdot \frac{C_p}{\text{EC}_{50} + C_p} \right) - K_{\text{OUT}} \cdot \text{Response} \quad (3)$$

$$f_{k_j|k_{j-1}} = B_{k_j|k_{j-1}} + \text{Response}(t) \quad (4)$$

where  $K_{\text{IN}}$  and  $K_{\text{OUT}}$  are the zero-order production rate and first-order removal rate constant of drug response, respectively. The  $K_{\text{OUT}}$  was set equal to  $K_{\text{IN}}$ .  $E_{\text{max}}$  is the maximal toxicity effect of the drug, and  $\text{EC}_{50}$  is the drug concentration

**Table III.** Parameter Estimates of the Final Myelosuppression Model and the Results of the Sampling Importance Resampling (SIR) Approach

Parameter	Estimate (RSE %) <sup>a</sup> (Shrinkage %)	Meaning of parameters
<b>Fixed effects</b>		
MTT (h)	158 (9.60)	Mean transit time
Circ <sub>0</sub> (10 <sup>9</sup> cells/l)	5.47 (11.2)	Baseline leukocyte count
$\gamma$	0.151 (22.3)	Feedback loop factor on the proliferation rate
SLP (L/mg)	0.0205 (19.9)	Slope of the linear drug-effect relationship
SP <sub>max</sub>	1.40 (17.6)	Maximum stimulatory effect of surgery stress on baseline proliferation rate
$k_{\text{CRS}}$ (1/h)	0.0362 (17.2)	First-order disappearance rate constant of the surgery stress effect
$A_{\text{deposit}}$ (10 <sup>9</sup> cells/l)	9.08 (18.3)	Number of leukocytes in the deposit pool
$k_{\text{release}}$ (1/h)	0.0535 (20.2)	First-order release rate constant associated with the deposit pool
$k_{\text{NACT}}$ (1/h)	0.01 (18.0)	First-order disappearance rate constant of the residual myelosuppressive effect of the neoadjuvant chemotherapy
<b>Inter-individual variability (IIV) (CV%)</b>		
Circ <sub>0</sub>	32.0 (27.8) [6.60]	
SP <sub>max</sub>	33.6 (28.3) [26.1]	
$A_{\text{deposit}}$	74.4 (28.6) [17.0]	
$k_{\text{release}}$	232 (29.8) [20.9]	
<b>Residual variability</b>		
Proportional error (%)	21.1 (19.1) [13.9]	

CV (%) is calculated according to  $\text{CV}(\%) = \sqrt{\exp(\omega^2) - 1} \times 100\%$ .  $\omega^2$ , the variance estimate in the log domain

<sup>a</sup>RSE, relative standard error, obtained from SIR



to give the half-maximal effect. The drug toxicity effect is implemented on  $K_{IN}$  as a stimulatory function.

The parameters were estimated with good precision and are reported on the logit scale in Table IV. The visual predictive check plot (Fig. 4) shows that the model described the time course for the incidence and severity of nephrotoxicity well.

### Simulation-Based Analysis

Since the observed leukopenia and leukocytosis in this study were short-lasting and not severe, the hematological toxicity was not the dose-limiting toxicity for dose regimen optimization. Hence, only the nephrotoxicity model was used for the simulations to explore the optimal treatment regimen. The 1000 virtual patients with randomly sampled PK parameters were assigned a fixed BSA of  $1.80 \text{ m}^2$  (median value of this study) and were given the normothermic or hyperthermic IPEC treatment. The impact of dose level and IPEC duration under normothermia on the time course of incidence and severity of nephrotoxicity is shown in Fig. 5.

As seen from the plot, at the low dose of  $75 \text{ mg/m}^2$ , the incidence and severity of nephrotoxicity are low with grade  $\geq 1$  and grade  $\geq 3$  nephrotoxicities less than 13.3% (maximum at day 1) and 6.9% (maximum at day 7), respectively. An extension of IPEC time from 1 to 2 h at this dose level would only lead to a marginal increase in the incidence of nephrotoxicity. When moving to the dose of  $100 \text{ mg/m}^2$ , the 1-h IPEC duration gave similar nephrotoxicity profiles to the low dose of  $75 \text{ mg/m}^2$  with an IPEC duration of 1.5 h, while IPEC durations of 1.5 and 2 h could lead to a maximum 9.6% (at day 4) and 12.9% (at day 7) of grade  $\geq 3$  nephrotoxicity,

**Table IV.** Parameter Estimates of the Final Nephrotoxicity Model and the Results of the Sampling Importance Resampling (SIR) Approach

Parameter	Final model Estimate (RSE %)	SIR results	
		Median	95% CI
$B_{110}$	-7.67 (14.9)	-7.74	(-9.63, -6.03)
$B_{210}$	-2.64 (36.7)	-2.77	(-4.95, -1.29)
$B_{111}$	-3.22 (34.2)	-3.24	(-5.04, -1.65)
$B_{211}$	-2.86 (23.8)	-2.89	(-4.31, -1.57)
$B_{112}$	11.0 (11.2)	11.6	(9.39, 13.7)
$B_{212}$	-14.1 (1.20)	-14.7	(-15.2, -14.2)
$B_{\geq 3 2}$	-1.21 (58.3)	-1.28	(-2.76, -0.32)
$B_{2 \geq 3}$	-5.45 (22.9)	-5.53	(-7.62, -3.55)
$E_{max}$	344 (42.7)	354	(182, 559)
$EC_{50}$ ( $\mu\text{g/ml}$ )	0.433 (29.3)	0.441	(0.294, 0.598)
$K_{IN}$ ( $1 \cdot \text{h}^{-1}$ )	0.00694 (32.0)	0.00689	(0.00447, 0.00986)

RSE, relative standard error; CI, confidence interval;  $B_{k_j|k_{j-1}}$ , intercept of the logit of the transition probability.  $B_{\geq 3|0}$ ,  $B_{\geq 3|1}$ ,  $B_{1|\geq 3}$ , and  $B_{0|\geq 3}$  were not estimated due to the fact that transition probabilities of  $0 \rightarrow \geq 3$ ,  $1 \rightarrow \geq 3$ ,  $\geq 3 \rightarrow 1$ , and  $\geq 3 \rightarrow 0$  were assumed to be zero.  $E_{max}$ , maximal toxicity effect of the drug;  $EC_{50}$ , the drug concentration to give the half-maximal effect;  $K_{IN}$ , zero-order production rate

respectively. With the high dose of  $120 \text{ mg/m}^2$ , the maximum incidence of grade  $\geq 3$  nephrotoxicity went from 7.1% (at day 7) to 16.9% (at day 4) when the treatment duration was extended from 1 to 2 h.

For the virtual patients with hyperthermic IPEC, the simulation results showed no clinically relevant differences in the time course of nephrotoxicity (Fig. S7 in Supplemental 2) compared with normothermic IPEC.

### DISCUSSION

Although the total platinum or ultrafiltrated platinum-based pharmacokinetics of cisplatin after (H)IPEC treatment have been widely reported in literature (31–33), only one study reported the summary PK parameters (based on non-compartmental analysis) of intact cisplatin in 10 patients who received 90 min HIPEC (34). The present study reported here describes the population pharmacokinetics of intact cisplatin under hyperthermic or normothermic IPEC in 50 patients. A two-compartment model was used to describe the disposition of intact cisplatin, which has also often been observed by many intraperitoneal or intravenous pharmacokinetic studies of cisplatin using total platinum or ultrafiltrated platinum concentrations (31–33,35). The typical absorption half-life in our study was 0.62 h. This was in the reported range of 0.18–1.66 h from earlier studies using total platinum or intact cisplatin (32,34,36), demonstrating that the use of total platinum or intact cisplatin does not lead to a marked difference in the estimation of the absorption parameters. But the difference in systemic half-life between intact cisplatin and total platinum was quite large: the typical systemic half-life (0.25 h) of intact cisplatin was 96- to 508-fold smaller than the terminal half-life (i.e., 24 to 127 h) of total platinum derived from cisplatin (37), indicating the great systemic pharmacokinetic difference between intact cisplatin and total platinum. Additionally, we found a high correlation between central volume of distribution and clearance, and this may indicate the presence of non-linearity due to the saturation of plasma protein binding for cisplatin.

The impact of hyperthermia on the cisplatin PKPD has not been reported previously. In our study, we found that hyperthermia leads to a faster absorption rate, also implying that less cisplatin is available locally in the peritoneum to exert its effect on the tumor nodules. For the small molecules in solution, the transmembrane absorption is permeability-limited and diffusion is the main driver for absorption (38). Basically, enhancing the temperature increases the molecule's movement speed; hence, diffusion happens faster. This may explain that a higher absorption rate was observed under hyperthermia compared with the normothermic condition. Also, hyperthermia may increase peritoneal blood flow, resulting in faster vascular clearance of cisplatin. However, the hyperthermic effect on the absorption rate only resulted in a slight increase in cisplatin plasma  $C_{max}$ , and no or clinically irrelevant differences in the toxicity profiles were identified compared with the normothermic group. The benefit of hyperthermia needs to be inspected by analyzing the tumor penetration and survival outcome of this trial, to be awaited from future observations.

Hematological toxicity such as neutropenia and leukopenia are common side effects of cisplatin-mediated

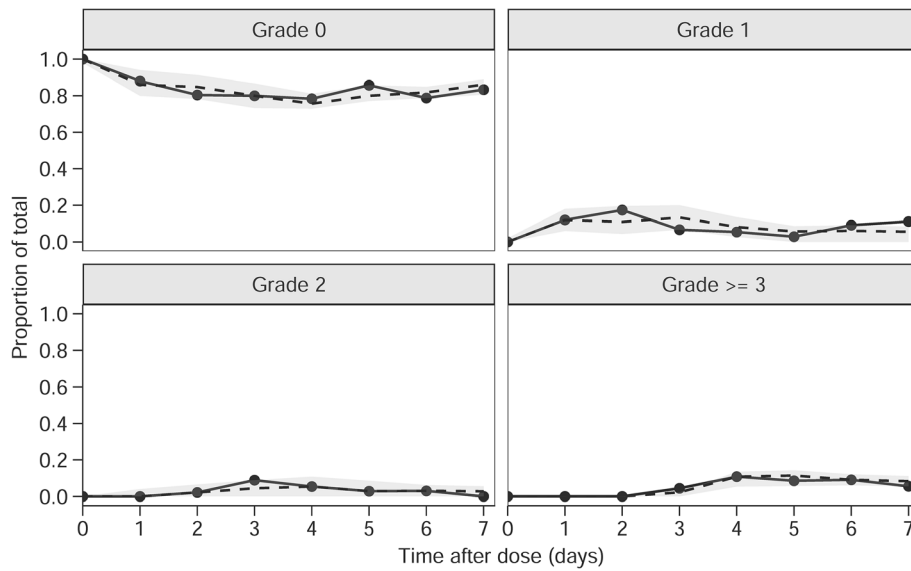


**Fig. 4.** Visual predictive checks of the final model for the time course of the probability and severity of nephrotoxicity. The solid lines represent the observed time course of each severity grade. The dashed lines represent the median time course of each severity grade from the model simulations, and the shaded areas are the 95% confidence intervals generated from simulations

myelosuppression (18). Previously, CTCAE grade 3 (severe) or 4 (life-threatening) hematological toxicities were found for intravenous administration of cisplatin in cancer patients (39). However, only a few cases of short-lasting mild or moderate leukopenia were observed in our cisplatin (H)IPEC-based treatment due to the rapid increase of leukocytes induced by surgery. The inflammatory cascade after surgery is associated with an increase of circulating granulopoiesis (e.g., neutrophilia and leukocytosis) whose effects include increased proliferation of granulocytic precursors, reduction of transit time through the granulocytic compartment, and release of (stored) mature cells from a marginated pool

within the bone marrow sinusoids (29). The mobilization of granulocytes from the bone marrow is thought to be the main contributor to the rapid increase in circulating granulocytes under stress and systemic inflammatory conditions (29,40). Recently, Pérez-Ruixo *et al.* reported a neutrophil dynamics model that accounts for the surgery-induced neutrophilia phenomena in peritoneal carcinomatosis patients treated with CRS and oxaliplatin-based HIPEC (30). In their model, the first two aforementioned pathophysiological mechanisms were taken into account by assuming that CRS increases the mitosis rate of proliferative cells and reduces the maturation time of neutrophil precursors in the bone marrow. During our

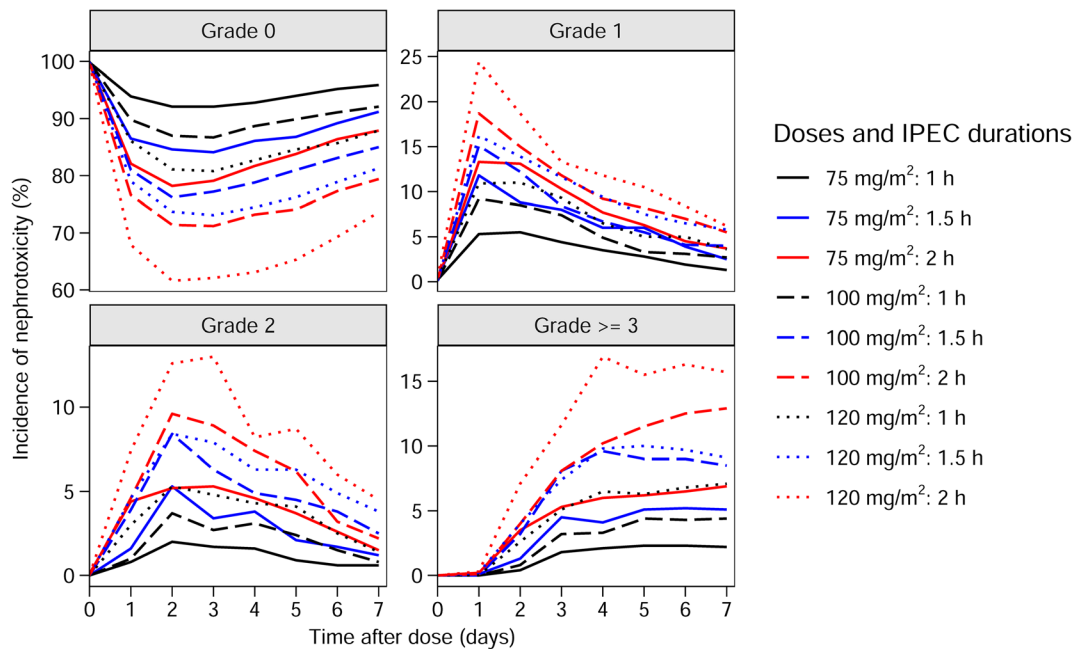


**Fig. 5.** Effect of cisplatin-based dose levels and intraoperative normothermic intraperitoneal chemoperfusion (IPEC) durations on the time course of nephrotoxicity incidence *via* simulations

leukocyte model development, all three aforementioned pathophysiological mechanisms were considered, and we found that the proliferation of leukocyte precursors and the mobilization of leukocytes from a deposit compartment (representing the marginated pool within the bone marrow) best described the rapid increase of leukocytes after CRS in the context of our dataset. It should be noted that our data did not support the estimation of the inverse mobilization of leukocytes from the circulating compartment to the deposit compartment. Therefore, the physiologically marginated pool was simplified with only the forward mobilization rate into the blood.

One way to evaluate the performance of the semi-mechanistic myelosuppression model is to check the consistency of system-related parameters ( $Circ_0$ , MTT, and  $\gamma$ ) with reported values. In our extended model, the estimated  $Circ_0$  was  $5.47 \times 10^9$  cells/l, which is in the physiological leukocyte range ( $4.0\text{--}11.0 \times 10^9$  cells/l). The estimated MTT value of 158 h is also in the reported range of 83.9–166 h (41) and was comparable with the values obtained from Pérez-Ruixo *et al.* (MTT: 144 h) (30) and from another paclitaxel- and carboplatin-based IV treatment study (MTT: 141 h) (42). The  $\gamma$  was estimated to be 0.151 (30), which is again similar with the value from Pérez-Ruixo *et al.* ( $\gamma$ : 0.155) and is in the reported  $\gamma$  range (0.101–0.26) (41). In addition, the surgical-stress parameter  $SP_{max}$  (1.4) on  $k_{prol(0)}$  in our study is somewhat different from the value from Pérez-Ruixo *et al.* (2.37). This may be explained by the fact that the surgery effect mechanisms we adopted were different from those in Pérez-Ruixo *et al.*, although the ultimate surgery effect on  $k_{prol(0)}$  was the same. The surgical parameter estimates may somehow differ based upon the underlying mechanisms implemented.

The commonly used nephrotoxicity markers of cisplatin are blood urea nitrogen, serum or plasma creatinine, and creatinine clearance. These markers are repeatedly measured over a period of time for each patient and are continuous data. In the clinic, these values are usually categorized and reported as ordered grades for facilitating straightforward interpretation, although this practice unnecessarily loses some information. In this study, we initially attempted to capture the time courses of serum creatinine in order to maximize the obtained information. Unfortunately, it turned out that modeling of the kinetics of serum creatinine is challenging due to the fact that the serum creatinine levels (Fig. S8 in Supplemental 2) were influenced by the mixture effects of the surgery-induced muscle loss (resulting in declined serum creatinine due to decreased production) and drug-induced kidney impairment (resulting in increased serum creatinine due to diminished elimination). We therefore switched to model the categorized data. The data categorization removes the “clinically irrelevant” variations and enables a more direct evaluation of nephrotoxicity.

Traditionally, the analysis of categorical toxicity data is mainly descriptive, such as only reporting the highest toxicity grade during the study and its associated percentage of patients, thereby neglecting the longitudinal dimension of toxicity data (43). Since the pioneering work by Sheiner in 1994, the field of modeling ordered categorical PD data has been growing rapidly and is frequently performed using the proportional odds model (44,45). However, the proportional

odds model is deemed not suitable for repeatedly measured categorical data when there are pronounced correlations between neighboring observations (46). In the present study, we applied a first-order mixed effects Markov model that successfully characterized the dynamics of longitudinal nephrotoxicity data. We showed that dose, AUC, and  $C_{max}$  are all significant predictors of the nephrotoxicity, and a quantitative relationship between the intact cisplatin concentration-time profile and the time course of nephrotoxicity was established. To a certain extent, our findings are in line with previous reports where the quantitative relationships between nephrotoxicity markers and intact cisplatin-based summary pharmacokinetic parameters (i.e., AUC and  $C_{max}$ ) were described after intravenous injection in rats and patients (47–49). Conversely, in a cisplatin-based HIPEC treatment study in peritoneal carcinomatosis patients, Cotte *et al.* (31) demonstrated no direct relationship between platinum-based AUC in the peritoneum or in plasma, and nephrotoxicity. The use of total platinum and not intact cisplatin in the study by Cotte *et al.* might have contributed to the lack of detection of the underlying relationship between drug exposure and nephrotoxicity. This may further highlight the importance of using intact cisplatin for meaningful PKPD analysis. However, it currently remains unknown which analytical measurement (parent platinum drug, total platinum, or the combination of them) is the best surrogate marker to identify the influential covariates and to predict drug responses, i.e., both the toxicity and efficacy. Future results are needed to answer this unresolved question.

The developed dynamic longitudinal nephrotoxicity model could be used as a valuable forecasting tool to provide the quantitative information for the management of side effects, as demonstrated in our simulation study for treatment optimization. However, a potential limitation of our nephrotoxicity model is that the actual perfusion duration was kept constant at 90 min. As a result, the developed PD model and estimated parameters such as transition probabilities were not validated at other durations. This may lead to some inaccuracies in the model predictions for other durations of (H)IPEC. During our treatment optimization, only the dose-limiting toxicity (i.e., nephrotoxicity) for cisplatin was considered; thereby, the predicted treatment regimens with minimal toxicity may not necessarily be associated with the optimal treatment outcome. Currently, there is no clear relationship between cisplatin-based (H)IPEC treatment regimen and the survival in ovarian cancer patients. Often, the clinical survival outcomes are subject to various influential factors such as disease state and surgery (50) and may require years to collect in order to infer a statistically significant conclusion. Hence, in the case of lacking efficacy data, it is rational to only use the dose-limiting toxicity model to guide the choice of an optimal treatment regimen. Our simulations suggest that a dose of  $75 \text{ mg/m}^2$  with an IPEC duration  $\leq 2 \text{ h}$  is a good treatment regimen in terms of minimal toxicity. This is partly confirmed by the observed toxicity data for the same dose with a duration of 1.5 h. When a high dose between 100 and  $120 \text{ mg/m}^2$  is to be administered, a (H)IPEC duration of 1 h is recommended to minimize the nephrotoxicity while providing relatively high local concentrations.

## CONCLUSION

We presented the PKPD models for the PK of unchanged cisplatin and the resulting adverse effects (myelosuppression and nephrotoxicity) in ovarian cancer patients under (H)IPEC treatment. The modeling work demonstrated that hyperthermic drug administration has a moderate effect on cisplatin's PK while does not lead to increased adverse effects compared with normothermic IPEC. Myelosuppression was not severe for cisplatin-based (H)IPEC. Nephrotoxicity was the major safety concern under (H)IPEC, and both the dose and IPEC duration should be carefully selected to achieve minimal nephrotoxicity.

## ACKNOWLEDGMENTS

The authors thank all study participants and their families. We also thank the clinical study team members at the different study sites.

## FUNDING INFORMATION

This work was supported by the Fund for Scientific Research – Flanders (FWO) (project number: G016915N).

## COMPLIANCE WITH ETHICAL STANDARDS

**Conflict of Interest** An Vermeulen is an employee of Johnson & Johnson and holds stock/stock options in the company. She is also a visiting Professor at Ghent University. Wim Ceelen is a senior clinical researcher from the Fund for Scientific Research – Flanders (FWO). The other authors have no competing interests to declare.

## REFERENCES

- Bray F, Ferlay J, Soerjomataram I, Siegel RL, Torre LA, Jemal A. Global cancer statistics 2018: GLOBOCAN estimates of incidence and mortality worldwide for 36 cancers in 185 countries. *CA Cancer J Clin*. 2018;68(6):394–424.
- de Bree E, Helm CW. Hyperthermic intraperitoneal chemotherapy in ovarian cancer: rationale and clinical data. *Expert Rev Anticancer Ther*. 2012;12(7):895–911.
- Tummala MK, Alagarsamy S, McGuire WP. Intraperitoneal chemotherapy: standard of care for patients with minimal residual stage III ovarian cancer? *Expert Rev Anticancer Ther*. 2008;8(7):1135–47.
- Polom K, Roviello G, Generali D, Marano L, Petrioli R, Marsili S, *et al*. Cytoreductive surgery and hyperthermic intraperitoneal chemotherapy for treatment of ovarian cancer. *Int J Hyperth*. 2016;32(3):298–310.
- Van Driel WJ, Koole SN, Sikorska K, Schagen van Leeuwen JH, Schreuder HW, Hermans RH, *et al*. Hyperthermic intraperitoneal chemotherapy in ovarian cancer. *N Engl J Med*. 2018;378(3):230–40.
- Van Driel WJ, Lok CA, Verwaal V, Sonke GS. The role of hyperthermic intraperitoneal intraoperative chemotherapy in ovarian cancer. *Curr Treat Options in Oncol*. 2015;16(4):14.
- Ceelen WP, Van Nieuwenhove Y, Van Belle S, Denys H, Pattyn P. Cytoreduction and hyperthermic intraperitoneal chemoperfusion in women with heavily pretreated recurrent ovarian cancer. *Ann Surg Oncol*. 2012;19(7):2352–9.
- Cowan RA, O'Ceirbhail RE, Zivanovic O, Chi DS. Current status and future prospects of hyperthermic intraoperative intraperitoneal chemotherapy (HIPEC) clinical trials in ovarian cancer. *Int J Hyperth*. 2017;33(5):548–53.
- de Bree E, Theodoropoulos PA, Rosing H, Michalakis J, Romanos J, Beijnen JH, *et al*. Treatment of ovarian cancer using intraperitoneal chemotherapy with taxanes: from laboratory bench to bedside. *Cancer Treat Rev*. 2006;32(6):471–82.
- Fujiwara K, Armstrong D, Morgan M, Markman M. Principles and practice of intraperitoneal chemotherapy for ovarian cancer. *Int J Gynecol Cancer*. 2007;17(1):1–20.
- Hettinga J, Konings A, Kampinga H. Reduction of cellular cisplatin resistance by hyperthermia—a review. *Int J Hyperth*. 1997;13(5):439–57.
- Takemoto M, Kuroda M, Urano M, Nishimura Y, Kawasaki S, Kato H, *et al*. The effect of various chemotherapeutic agents given with mild hyperthermia on different types of tumours. *Int J Hyperth*. 2003;19(2):193–203.
- Sugarbaker PH. Peritonectomy procedures. *Surg Oncol Clin N Am*. 2003;12(3):703–27.
- Hanada K, Nishijima K, Ogata H, Atagi S, Kawahara M. Population pharmacokinetic analysis of cisplatin and its metabolites in cancer patients: possible misinterpretation of covariates for pharmacokinetic parameters calculated from the concentrations of unchanged cisplatin, ultrafiltered platinum and total platinum. *Jpn J Clin Oncol*. 2001;31(5):179–84.
- Farris FF, King FG, Dedrick RL, Litterst CL. Physiological model for the pharmacokinetics of cis-dichlorodiammineplatinum (II)(DDP) in the tumored rat. *J Pharmacokinet Biopharm*. 1985;13(1):13–39.
- Alderden RA, Hall MD, Hambley TW. The discovery and development of cisplatin. *J Chem Educ*. 2006;83(5):728.
- Yao X, Panichpisal K, Kurtzman N, Nugent K. Cisplatin nephrotoxicity: a review. *Am J Med Sci*. 2007;334(2):115–24.
- Barabas K, Milner R, Lurie D, Adin C. Cisplatin: a review of toxicities and therapeutic applications. *Vet Comp Oncol*. 2008;6(1):1–18.
- Reichman TW, Cracchiolo B, Sama J, Bryan M, Harrison J, Pliner L, *et al*. Cytoreductive surgery and intraoperative hyperthermic chemoperfusion for advanced ovarian carcinoma. *J Surg Oncol*. 2005;90(2):51–6.
- Königsrainer I, Horvath P, Struller F, Grischke EM, Wallwiener D, Königsrainer A, *et al*. Cytoreductive surgery and hyperthermic intraperitoneal chemotherapy in recurrent epithelial ovarian cancer with peritoneal metastases: a single centre experience. *Langenbeck's Arch Surg*. 2014;399(5):589–94.
- Batista TP, Badiglian Filho L, Leão CS. Exploring flow rate selection in HIPEC procedures. *Rev Col Bras Cir*. 2016;43(6):476–9.
- Campbell AB, Kalman SM, Jacobs C. Plasma platinum levels: relationship to cisplatin dose and nephrotoxicity. *Cancer Treat Rep*. 1983;67(2):169–72.
- Reece PA, Stafford I, Russell J, Khan M, Gill P. Creatinine clearance as a predictor of ultrafilterable platinum disposition in cancer patients treated with cisplatin: relationship between peak ultrafilterable platinum plasma levels and nephrotoxicity. *J Clin Oncol*. 1987;5(2):304–9.
- Klaver YL, Hendriks T, Lomme RM, Rutten HJ, Bleichrodt RP, de Hingh IH. Hyperthermia and intraperitoneal chemotherapy for the treatment of peritoneal carcinomatosis: an experimental study. *Ann Surg*. 2011;254(1):125–30.
- Carlier C, Laforce B, Van Malderen SJ, Gremontprez F, Tucoulou R, Villanova J, *et al*. Nanoscopic tumor tissue distribution of platinum after intraperitoneal administration in a xenograft model of ovarian cancer. *J Pharm Biomed Anal*. 2016;131:256–62.
- Alvovsky I, Bepalov V, Kireeva G. Cisplatin in NIPEC or HIPEC? *Ann Surg*. 2018;29(suppl\_8):mdy268.020.
- Xie F, Colin P, Van Bocxlaer J. Zwitterionic hydrophilic interaction liquid chromatography-tandem mass spectrometry with HybridSPE-precipitation for the determination of intact cisplatin in human plasma. *Talanta*. 2017;174:171–8.
- Friberg LE, Henningson A, Maas H, Nguyen L, Karlsson MO. Model of chemotherapy-induced myelosuppression with parameter consistency across drugs. *J Clin Oncol*. 2002;20(24):4713–21.

29. Summers C, Rankin SM, Condliffe AM, Singh N, Peters AM, Chilvers ER. Neutrophil kinetics in health and disease. *Trends Immunol.* 2010;31(8):318–24.
30. Pérez-Ruixo C, Valenzuela B, Peris JE, Bretcha-Boix P, Escudero-Ortiz V, Farré-Alegre J, *et al.* Neutrophil dynamics in peritoneal carcinomatosis patients treated with cytoreductive surgery and hyperthermic intraperitoneal oxaliplatin. *Clin Pharmacokinet.* 2013;52(12):1111–25.
31. Cotte E, Colomban O, Guitton J, Tranchand B, Bakrin N, Gilly FN, *et al.* Population pharmacokinetics and pharmacodynamics of cisplatin during hyperthermic intraperitoneal chemotherapy using a closed abdominal procedure. *J Clin Pharmacol.* 2011;51(1):9–18.
32. Royer B, Jullien V, Guardiola E, Heyd B, Chauffert B, Kantelip JP, *et al.* Population pharmacokinetics and dosing recommendations for cisplatin during intraperitoneal peroperative administration: development of a limited sampling strategy for toxicity risk assessment. *Clin Pharmacokinet.* 2009;48(3):169–80.
33. Royer B, Kalbacher E, Onteniente S, Jullien V, Montange D, Piedoux S, *et al.* Intraperitoneal clearance as a potential biomarker of cisplatin after intraperitoneal perioperative chemotherapy: a population pharmacokinetic study. *Br J Cancer.* 2012;106(3):460–7.
34. Cashin PH, Ehrsson H, Wallin I, Nygren P, Mahteme H. Pharmacokinetics of cisplatin during hyperthermic intraperitoneal treatment of peritoneal carcinomatosis. *Eur J Clin Pharmacol.* 2013;69(3):533–40.
35. Urien S, Lokiec F. Population pharmacokinetics of total and unbound plasma cisplatin in adult patients. *Br J Clin Pharmacol.* 2004;57(6):756–63.
36. Royer B, Guardiola E, Polycarpe E, Hoizey G, Delroeux D, Combe M, *et al.* Serum and intraperitoneal pharmacokinetics of cisplatin within intraoperative intraperitoneal chemotherapy: influence of protein binding. *Anti-Cancer Drugs.* 2005;16(9):1009–16.
37. O'dwyer PJ, Stevenson JP, Johnson SW. Clinical pharmacokinetics and administration of established platinum drugs. *Drugs.* 2000;59(4):19–27.
38. Borbás E, Sinkó B, Tsinman O, Tsinman K, Ev K, Démuth B, *et al.* Investigation and mathematical description of the real driving force of passive transport of drug molecules from supersaturated solutions. *Mol Pharm.* 2016;13(11):3816–26.
39. Specenier PM, Ciuleanu T, Latz JE, Musib LC, Darstein CL, Vermorken JB. Pharmacokinetic evaluation of platinum derived from cisplatin administered alone and with pemetrexed in head and neck cancer patients. *Cancer Chemother Pharmacol.* 2009;64(2):233–41.
40. Burdon PC, Martin C, Rankin SM. Migration across the sinusoidal endothelium regulates neutrophil mobilization in response to ELR+ CXC chemokines. *Br J Haematol.* 2008;142(1):100–8.
41. Evans ND, Cheung SA, Yates JW. Structural identifiability for mathematical pharmacology: models of myelosuppression. *J Pharmacokinet Pharmacodyn.* 2018;45(1):79–90.
42. Joerger M, Huitema AD, Richel DJ, Dittrich C, Pavlidis N, Briassoulis E, *et al.* Population pharmacokinetics and pharmacodynamics of paclitaxel and carboplatin in ovarian cancer patients: a study by the European organization for research and treatment of cancer-pharmacology and molecular mechanisms group and new drug development group. *Clin Cancer Res.* 2007;13(21):6410–8.
43. Hénin E, You B, VanCutsem E, Hoff P, Cassidy J, Twelves C, *et al.* A dynamic model of hand-and-foot syndrome in patients receiving capecitabine. *Clin Pharmacol Ther.* 2009;85(4):418–25.
44. Schindler E, Karlsson MO. A minimal continuous-time Markov pharmacometric model. *AAPS J.* 2017;19(5):1424–35.
45. Sheiner LB. A new approach to the analysis of analgesic drug trials, illustrated with bromfenac data. *Clin Pharmacol Ther.* 1994;56(3):309–22.
46. Zingmark P-H, Kågedal M, Karlsson MO. Modelling a spontaneously reported side effect by use of a Markov mixed-effects model. *J Pharmacokinet Pharmacodyn.* 2005;32(2):261–81.
47. Nagai N, Kinoshita M, Ogata H, Tsujino D, Wada Y, Someya K, *et al.* Relationship between pharmacokinetics of unchanged cisplatin and nephrotoxicity after intravenous infusions of cisplatin to cancer patients. *Cancer Chemother Pharmacol.* 1996;39(1–2):131–7.
48. Nagai N, Ogata H. Quantitative relationship between pharmacokinetics of unchanged cisplatin and nephrotoxicity in rats: importance of area under the concentration-time curve (AUC) as the major toxicodynamic determinant in vivo. *Cancer Chemother Pharmacol.* 1997;40(1):11–8.
49. Hanada K, Asano K, Nishimura T, Chimata T, Matsuo Y, Tsuchiya M, *et al.* Use of a toxicity factor to explain differences in nephrotoxicity and myelosuppression among the platinum antitumour derivatives cisplatin, carboplatin and nedaplatin in rats. *J Pharm Pharmacol.* 2008;60(3):317–22.
50. Le Saux O, Decullier E, Freyer G, Glehen O, Bakrin N. Long-term survival in patients with epithelial ovarian cancer following cytoreductive surgery and hyperthermic intraperitoneal chemotherapy (HIPEC). *Int J Hypertherm.* 2018;35(1):652–7.

**Publisher's Note** Springer Nature remains neutral with regard to jurisdictional claims in published maps and institutional affiliations.